npj | biofilms and microbiomes

Article

Published in partnership with Nanyang Technological University

https://doi.org/10.1038/s41522-024-00558-w

Natural killer cell effector function is critical for host defense against alcohol-associated bacterial pneumonia

Daniel N. Villageliu[1], Kelly C. Cunningham[1], Deandra R. Smith[2], Daren L. Knoell[2], Mason Mandolfo[1], Todd A. Wyatt[1,3,4] & Derrick R. Samuelson[1,5]

Alcohol use is an independent risk factor for the development of bacterial pneumonia due, in part, to impaired mucus-facilitated clearance, macrophage phagocytosis, and recruitment of neutrophils. Alcohol consumption is also known to reduce peripheral natural killer (NK) cell numbers and compromise NK cell cytolytic activity, especially NK cells with a mature phenotype. However, the role of innate lymphocytes, such as NK cells during host defense against alcohol-associated bacterial pneumonia is essentially unknown. We have previously shown that indole supplementation mitigates increases in pulmonary bacterial burden and improves pulmonary NK cell recruitment in alcohol-fed mice, which were dependent on aryl hydrocarbon receptor (AhR) signaling. Employing a binge-on-chronic alcohol-feeding model we sought to define the role and interaction of indole and NK cells during pulmonary host defense against alcohol-associated pneumonia. We demonstrate that alcohol dysregulates NK cell effector function and pulmonary recruitment via alterations in two key signaling pathways. We found that alcohol increases transforming growth factor beta (TGF-β) signaling while suppressing AhR signaling. We further demonstrated that NK cells isolated from alcohol-fed mice have a reduced ability to kill *Klebsiella pneumoniae*. NK cell migratory capacity to chemokines was also significantly altered by alcohol, as NK cells isolated from alcohol-fed mice exhibited preferential migration in response to CXCR3 chemokines but exhibited reduced migration in response to CCR2, CXCR4, and CX3CR1 chemokines. Together this data suggests that alcohol disrupts NK cell-specific TGF-β and AhR signaling pathways leading to decreased pulmonary recruitment and cytolytic activity thereby increasing susceptibility to alcohol-associated bacterial pneumonia.

Alcohol use disorder (AUD) is an established risk factor for bacterial pneumonia and alcohol misuse carries a ten-fold increase in the likelihood of pneumococcal pneumonia, as well as a four-fold increase in mortality[1,2]. Alcohol ingestion is also associated with infection by other highly virulent respiratory pathogens including *Klebsiella pneumoniae*. Infection with *K. pneumoniae* carries a mortality almost double that of AUD patients infected by other pathogens and *K. pneumoniae* infections have historically been overrepresented in pneumonia patients with AUD[2,3]. A variety of mechanisms contribute to the increased risk of pneumonia in subjects with an AUD including decreased mucus-facilitated clearance of invading pathogens and pulmonary immune responses[4]. Though the above mechanisms are well established, our research has demonstrated the importance of other novel mechanisms, which derive from alterations to the composition and function of the gut microbiota. Precisely, we demonstrated that alcohol-associated dysbiosis increases susceptibility to *Klebsiella* pneumonia, independent of alcohol consumption[5].

[1]Department of Internal Medicine, Division of Pulmonary, Critical Care, & Sleep, University of Nebraska Medical Center, Omaha, NE, USA. [2]Department of Pharmacy Practice and Science, College of Pharmacy, University of Nebraska Medical Center, Omaha, NE, USA. [3]Department of Environmental, Agricultural and Occupational Health, College of Public Health, University of Nebraska Medical Center, Omaha, NE, USA. [4]Department of Veterans Affairs Nebraska, University of Nebraska Medical Center, Western Iowa Health Care System, Omaha, NE, USA. [5]Nebraska Food for Health Center, University of Nebraska-Lincoln, Lincoln, NE, USA. e-mail: derrick.samuelson@unmc.edu

Marked changes in pulmonary host defense were associated with alcohol-dysbiotic mice, including an increase in pulmonary inflammatory cytokines and a decrease in the number of immune cells (CD4+ and CD8 + T-cells) in the lung cells following *Klebsiella* infection. However, contrary to the pulmonary host response, a marked increase in immune cell counts was seen within the intestinal tract, which suggests that GI T-cell sequestration or dysregulated immune cell trafficking may impair pulmonary host defense[5]. Similarly, we found that prophylactic treatment with indole (a microbial-specific metabolite), or a cocktail of probiotics reduced both pulmonary and splenic bacterial burden, improved host immune responses, and facilitated pulmonary trafficking of immune cells. All of these were, in part, driven by aryl hydrocarbon receptors (AhR), as inhibition of AhR mitigated the protective effects. Further, indole increased the frequency of IL-22 immune cells in the lungs and small intestine, and enhanced pulmonary recruitment of $CD45^+$ cells, particularly $CD3^+$ T-cells and $NK1.1^+$ natural killer (NK) cells[6].

Here we demonstrate that alcohol dysregulates NK cell effector function and pulmonary recruitment via alterations in two key signaling pathways. We found that alcohol increases transforming growth factor beta (TGF-β1) signaling while suppressing AhR signaling. We further demonstrate that NK cells isolated from alcohol-fed mice have a reduced ability to kill *Klebsiella pneumoniae*. NK cell migratory capacity to chemokines was also significantly altered by alcohol, as NK cells isolated from alcohol-fed mice exhibited preferential migration in response to CXCR3 chemokines but exhibited reduced migration in response to CCR2, CXCR4, and CX3CR1 chemokines. Together this data suggests that alcohol disrupts NK cell-specific TGF-β1 and AhR signaling pathways leading to decreased pulmonary recruitment and cytolytic activity thereby increasing susceptibility to alcohol-associated bacterial pneumonia.

Results

NK cells are required for indole's protective effects on pulmonary bacterial burden

Our previous data demonstrated that indole supplementation during alcohol consumption alleviates alcohol-associated impairments in pulmonary host defense against bacterial pneumonia[6]. Further, indole treatment restored pulmonary immune cell recruitment. However, it is unknown if indole works directly or indirectly on immune cells. Here we sought to investigate whether indole's ability to mitigate the increased risk of alcohol-associated pneumonia was dependent on NK cells. Specifically, we depleted NK cells with a monoclonal antibody against NK1.1, which led to a greater than 95% depletion of pulmonary NK cells (Fig. 1A). The percentage of pulmonary CD3 + NK1.1 + NKT cells was also decreased in treated mice (Fig. 1B). Our representative gating strategy for NK cell depletion is shown in Fig. 1C. We first assessed the requirement of NK cells in indole-treated mice to reduce the susceptibility to *K. pneumoniae*. Alcohol-fed mice had a higher pulmonary burden of *K. pneumoniae* 48 h. post-infection compared to control mice (Fig. 1D). As seen previously, indole treatment reduced pulmonary *K. pneumoniae* burden in alcohol-fed mice (Fig. 1D). However, in alcohol-fed NK cell-depleted mice indole treatment failed to mitigate pulmonary *K. pneumoniae* burden (Fig. 1D). Previously, we observed that indole treatment improves epithelial permeability in alcohol-fed mice yet is unknown if NK cells are involved in this process. We examined mucosal permeability following *K. pneumoniae* infection in alcohol-fed NK cell-depleted mice treated with indole. Marked increases in both pulmonary and intestinal permeability were seen in alcohol-fed mice, as determined by increases in the circulating levels of surfactant protein-D (SDP-1; a biomarker of lung damage)[7], and intestinal fatty-acid binding protein (IFABP; a biomarker of intestinal damage)[8,9], respectively (Fig. 1E, F). Alcohol-fed mice treated with indole exhibited reduced SDP-1 and IFABP levels and

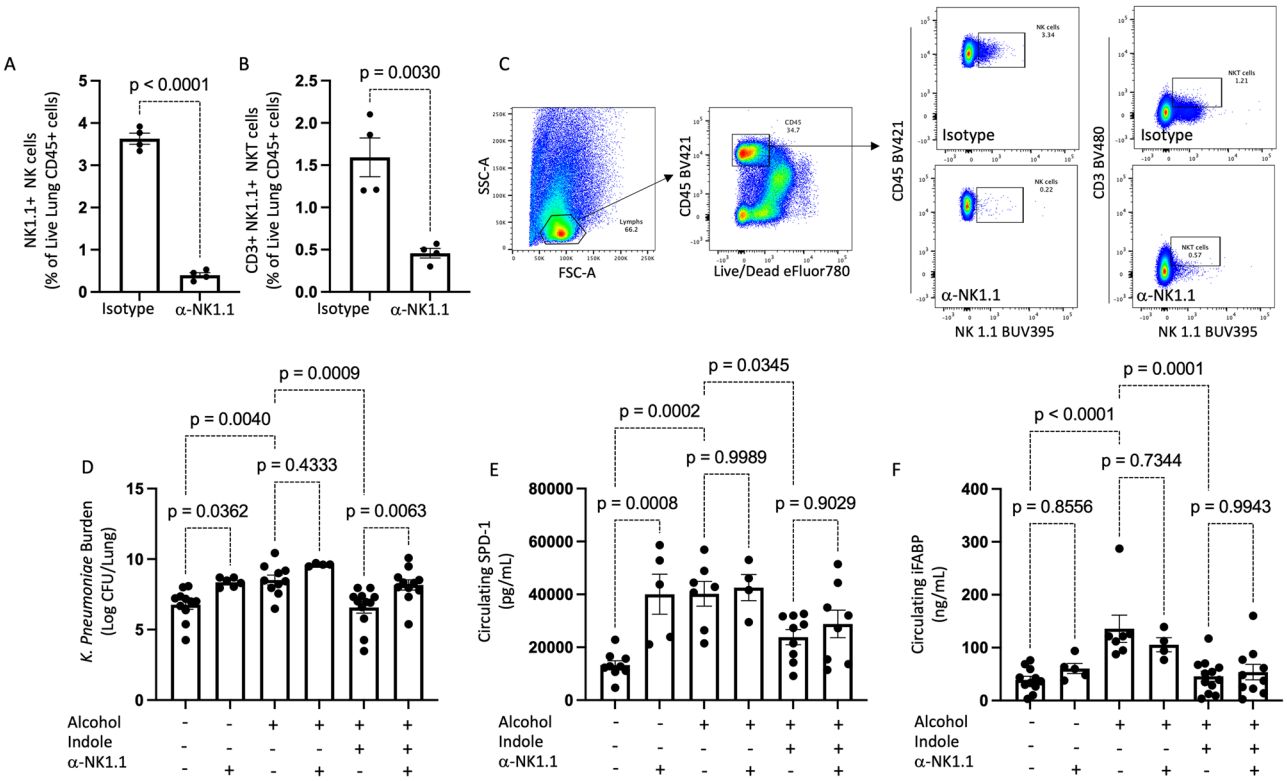

Fig. 1 | NK cells are required for optimal host defense against alcohol-associated pneumoniae. A Percentage of pulmonary NK cells and (**B**) T-cells following NK1.1 depletion. **C** Representative gating strategy. **D** *K. pneumoniae* lung burden at 48 h. post-infection in binge-on-chronic alcohol-treated mice. **E** Circulating levels of surfactant protein D1 (SPD-1) in binge-on-chronic alcohol-treated mice 48 h. post infection. **F** Circulating levels of intestinal fatty acid binding protein (iFABP) in binge-on-chronic alcohol-treated mice 48 h. post-infection; *p* values are indicated in the figure by one-way ANOVA with Sidak's multiple comparison. *N* = 10–12 mice/group derived from 2 independent experiments. *N* = 4–6 mice/group for the alcohol-fed or pair-fed with NK depletion derived from 1 experiment.

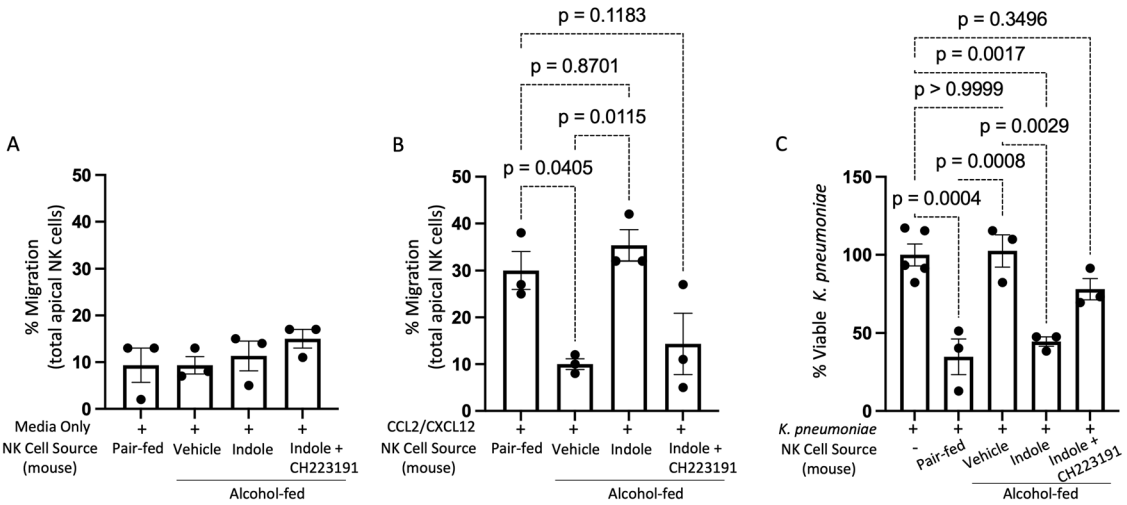

Fig. 2 | Alcohol impairs NK cell migratory capacity and bactericidal activity. Mouse primary NK cells were collected from alcohol-fed and treated mice and added to the apical side of a Transwell with migration assessed in response to (**A**) media alone, and (**B**) media with CCL2/CXCL12 following 5 h of incubation. **C** Primary NK cells were harvested from control and binge-on-chronic alcohol-fed mice with and without treatment. NK cells were then incubated with *K. pneumoniae* for 3 h. and bacterial viability was determined by serial dilution. *p*-values as determined by one-way ANOVA with Sidak's multiple comparisons are shown in the figure. $N = 3$ wells of primary NK cells/group (6 mice/group, NK cells per 2 mice were pooled).

were indistinguishable from control-fed mice after infection with *K. pneumoniae* (Fig. 1E, F). Interestingly, depletion of NK cells had no effect on the indole's ability to mitigate alcohol-induced mucosal permeability (Fig. 1E, F). This data suggests that NK cells contribute to reduced pulmonary bacterial burden in indole-treated mice. Further, this data suggests that indole may work both directly on NK cells, as well as other systems and cell types, as improvements in mucosal permeability are still preserved in NK cell-depleted mice.

Alcohol impairs NK cell migratory capacity

Our previous data demonstrated that indole supplementation during alcohol consumption restored pulmonary NK cell recruitment[6]. However, whether this effect was due to alterations in NK cell function or changes in chemokine production in the lungs is unknown. Here we sought to characterize the functional capacity of primary NK cells isolated from pair-fed mice, alcohol-fed mice, alcohol-fed mice treated with indole, as well as mice treated with the AhR inhibitor CH223191. NK cells were purified by negative selection, allowing us to examine functional characteristics including migration and bactericidal capacity. Primary NK cells isolated from alcohol-fed and treated mice exhibited no baseline differences in migratory capacity (Fig. 2A). However, NK cells isolated from alcohol-fed mice have a significantly reduced ability to migrate in response to the chemokines CCL2 and CXCL12 (Fig. 2B). CCL2 and CXCL12 are both strong chemo-attractants for NK cells[10]. Conversely, primary NK cells isolated from control animals retain the ability to migrate towards CCL2 and CXCL12. Furthermore, alcohol-associated impairments in migration can be overcome by the addition of the AhR agonist indole (Fig. 2B). The effect of indole is also mediated through the AhR receptor as the addition of the AhR antagonist CH223191 blocks the effects of indole (Fig. 2B).

Additionally, NK cells isolated from alcohol-fed mice have a significantly reduced ability to kill *Klebsiella pneumoniae* in co-culture experiments (Fig. 2C). Like the migration data, primary NK cells isolated from pair-fed animals retain the ability to kill *K. pneumoniae*. The alcohol-associated impairments in bactericidal capacity were also mitigated by the addition of the AhR agonist indole (Fig. 2C). The effect of indole was likewise dependent on AhR activation, as CH223191 blocks the effects of indole on NK cell bactericidal capacity (Fig. 2C).

Alcohol increases pulmonary and systemic TGF-β levels

The effects of alcohol on NK cell function suggest that alcohol consumption is associated with a highly immunosuppressive environment for NK cells. We sought to investigate systemic and pulmonary levels of TGF-β1, a potent immunosuppressive cytokine on NK cell function. Alcohol-fed mice exhibited marked increases in the levels of TGF-β1 in both serum and lung tissue (Fig. 3A, B, respectively), which is consistent with previous reports[11]. The administration of indole suppresses the alcohol-associated increases in TGF-β1 levels which was, in part, dependent on AhR activation. Specifically, in the presence of the AhR inhibitor CH223191, indole supplementation did not affect systemic or lung levels of TGF-β1 (Fig. 3A, B).

Additionally, we sought to evaluate the systemic and pulmonary levels of IL-22, a major cytokine downstream of AhR activation[12]. IL-22 is also involved in wound healing and in the protection against microbial infections[12–15]. Alcohol-fed mice exhibited marked decreases in the levels of IL-22 in both serum and lung tissue (Fig. 3C, D, respectively). Administration of indole suppressed the alcohol-associated decrease in IL-22 levels and was dependent, in part, on AhR activation (Fig. 3C, D, respectively).

Manipulation of TGF-β or AhR signaling pathways alters pneumonia outcomes in alcohol-fed mice

Divergent TGF-β and AhR signaling associated with alcohol consumption suggests that alcohol use shifts host defense pathways to an immunosuppressive phenotype (TGF-β) while decreasing immune regulatory/stimulatory pathways (AhR). As such, we sought to pharmacologically manipulate both signaling pathways to alter the host response to bacterial infection. Specifically, cohorts of female mice were randomized into the following groups: (1) alcohol + vehicle, (2) alcohol + indole (20 mg/kg), (3) alcohol + indole + CH-223191 (AhR inhibitor; 10 mg/kg), (4) alcohol + anti-TGF-β1 (10 mg/kg), (5) alcohol + TGF-β1 (0.5 μg/g), (6) pair-fed + vehicle, (7) pair-fed + TGF-β 1 (0.5 μg/g), (8) pair-fed + indole (20 mg/kg), (9) pair-fed + indole + CH-223191 (10 mg/kg), and (10) pair-fed + anti-TGF-β1 (10 mg/kg). Figure 4A depicts our experimental schema. We first assessed pulmonary bacterial burden 48 h post-infection in all mice. Alcohol-fed mice exhibited a marked increase in pulmonary bacterial burden relative to pair-fed mice (Fig. 4B). Similarly, pair-fed mice treated with exogenous TGF-β1 or alcohol-fed mice treated with indole and the AhR inhibitor CH223191 exhibited a significant increase in pulmonary bacterial burden compared to pair-fed mice (Fig. 4B). Conversely,

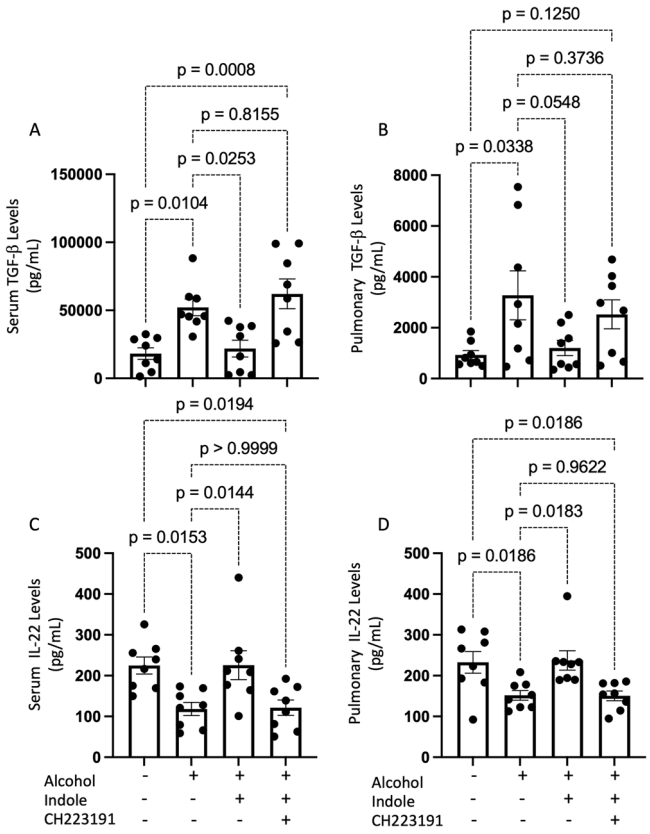

Fig. 3 | Alcohol increases pulmonary and circulating levels of TGF-β but decreases IL-22 levels following bacterial pneumonia. A Pulmonary TGF-β1 levels, **B** systemic TGF-β1 levels, as well as (**C**) pulmonary IL-22 levels, and (**D**) systemic IL-22 levels in binge-on-chronic alcohol-fed mice with and without treatment following *K. pneumoniae* infection. All graphs are 48 h. post infection; *p* values are indicated in the figure, as determined by one-way ANOVA with Sidak's multiple comparisons. $N = 8$ mice/group derived from 2 independent experiments.

administration of indole or the administration of anti-TGF-β1 monoclonal antibodies effectively reversed the detrimental effects of alcohol, by reducing the pulmonary bacterial burden to levels like those observed in pair-fed mice (Fig. 4B). Similarly, bacterial dissemination (Fig. 4C) was dependent on a balance of increased AhR activity and decreased TGF-β1 signaling, in line with the pulmonary results. These data also demonstrated that exogenous TGF-β1 did not act synergistically or additively to alcohol-feeding alone.

We also evaluated the pulmonary NK cell population following bacterial pneumonia. Our flow cytometry gating strategy for all NK cell populations is shown in Supplementary Fig. 1. Alcohol-fed mice, mice treated with the AhR inhibitor CH22319, and pair-fed mice treated with exogenous TGF-β1 exhibited a significant decrease in the percentage and number of pulmonary NK cells (Fig. 5A and Supplementary 2A). However, indole or anti-TGF-β1 monoclonal antibody treatment effectively reversed the detrimental effects of alcohol, by increasing the percentage and number of pulmonary NK cells (Fig. 5A and Supplementary 2A). We also found that the percentage and number of pulmonary NK cells that were AhR+ was lower in the lungs of alcohol-fed mice, alcohol-fed mice treated plus indole and CH22319, as well as pair-fed mice treated with TGF-β1 (Fig. 5B and Supplementary 2B). Conversely, the percentage and number of pulmonary NK cells that were TFGβR1+ were higher in the lungs of alcohol-fed mice, alcohol-fed mice treated plus indole and CH22319, as well as pair-fed mice treated with TGF-β1 (Fig. 5C and Supplementary 2C). These trends were reversed in pair-fed mice, as well as alcohol-fed mice treated with indole or the anti-TGF-β1 monoclonal antibody (Fig. 5B, C, and Supplementary 2B, C). We also evaluated the number of pulmonary NK cells with nuclear AhR (active form) using imaging flow cytometry. Administration of either exogenous recombinant TGF-β1 to control animals or alcohol decreased the percentage and number of NK cells with nuclear AhR (Fig. 5D and Supplementary 2D). However, pair-fed mice, as well as alcohol-fed mice treated with indole or the anti-TGF-β1 monoclonal antibody, exhibited a significant increase in the percentage and number of NK cells with nuclear AhR, compared to their respective controls (Fig. 5D and Supplementary 2D). Further, as expected, the AhR receptor antagonist CH223191 completely abolished the translocation of the AhR complex to the nucleus (Fig. 5D and Supplementary 2D).

Finally, NK cells were evaluated based on the 4-stage model of maturation using CD27, and CD11b markers[16]. Specifically, NK cells were grouped into CD11b−CD27−, CD11b−CD27+, CD11b+CD27+, and CD11b+CD27− where each step indicates the acquisition of NK cell effector functions and maturation. The percentage or number of stage 1, 2, or 3 NK cells were not significantly affected by alcohol consumption or by any of the exogenous treatments (Fig. 6A–C, and Supplementary 3A–C). Conversely, marked effects were seen in the percentage and number of stage 4 NK cells in the lungs of mice post-infection (Fig. 6D and Supplementary 3D). Specifically, administration of either TGF-β1 or alcohol decreased the percentage and number of stage 4 NK cells (Fig. 6D and Supplementary 3D). These trends were reversed in pair-fed mice, as well as alcohol-fed mice treated with indole or the anti-TGF-β1 monoclonal antibody, as these mice exhibited a significant increase in the percentage and number of pulmonary stage 4 NK cells, compared to their respective controls (Fig. 6D and Supplementary 3D).

Alcohol and TGF-β treatment increases pulmonary inflammation and epithelial leak

Histopathologic findings were consistent with observations for pulmonary bacterial burden and immune infiltration (Fig. 7). Specifically, we observed a significant increase in inflammatory scores for mice treated with alcohol ($p = 0.0091$) and TGF-β1. Inflammation was reduced to baseline by the addition of anti-TGF-β1 monoclonal antibody treatment, or indole supplementation. However, reduced inflammation by indole supplementation was not observed if indole was co-administered with the AhR inhibitor CH223191. Aggregation patterns mirrored inflammatory scores with increased aggregates with alcohol, TGF-β1, and alcohol/AhR inhibition treatments, however, these findings did not reach significance (Fig. 7).

We also observed that alcohol and TGF-β1 have several potentially detrimental effects on epithelial integrity. Consistent with our previous work, epithelial barrier function was impaired in the presence of either ethanol or TGF-β. Circulating levels of intestinal iFABP (Fig. 8A) and pulmonary SPD-1 (Fig. 8B) were increased, suggesting that barrier integrity was decreased by these treatments and contributing to immune burden via epithelial leakiness (Fig. 8). We further confirmed the effectiveness of recombinant TGF-β1 or anti-TGF-β1 monoclonal antibody treatment by measuring the levels of circulating TGF-β1. We confirmed that the exogenous administration of TGF-β1 utilized in our experiment increased TGF-β1 levels similar to alcohol-treated animals (Fig. 8C). Interestingly, we also observed that the AhR agonist indole was able to decrease the circulating levels of TGF-β1, which could be due, in part, to improved epithelial integrity.

Alcohol and TGF-β treatment significantly impair NK cell function

We then tested the influence of alcohol and TGF-β1 on NK cell trafficking, NK bactericidal capacity, and production of antibacterial products. Specifically, circulating and splenic NK cells were isolated from the following groups of mice: (1) alcohol + vehicle, (2) alcohol + indole (20 mg/kg), (3) alcohol + indole + CH-223191 (AhR inhibitor; 10 mg/kg), (4) alcohol + anti-TGF-β1 (10 mg/kg), (5) alcohol + TGF-β1 (0.5 μg/g), (6) pair-fed + vehicle, (7) pair-fed + TGF-β1 (0.5 μg/g), (8) pair-fed + indole (20 mg/kg), (9) pair-fed + indole + CH-223191 (10 mg/kg), and (10) pair-fed + anti-TGF-β1 (10 mg/kg). Circulating and splenic NK cells from two mice per treatment group (6–7 mice/group/exp, in vitro functional data from 2 independent experiments with a total of 6–7 wells of primary NK cells per

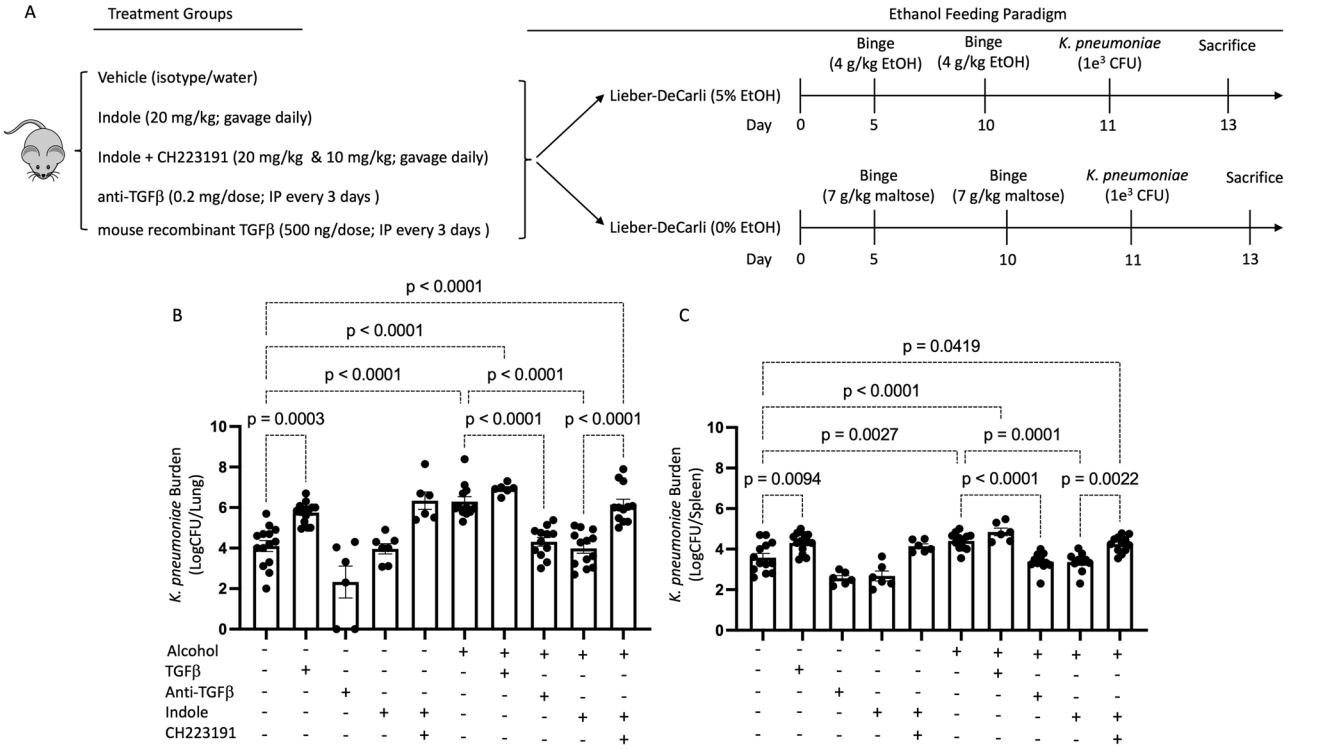

Fig. 4 | Host defense against alcohol-associated bacterial pneumonia requires activated AhR and decreased TGF-b signaling. A Overview of the dosing regimen for animals treated with indole, recombinant TGF-β1, anti-TGF-β1, and the AhR antagonist CH223191. *K. pneumoniae* (**B**) lung and (**C**) splenic burden at 48 h. post-infection in binge-on-chronic alcohol-treated mice. *p* values are indicated in the figure by one-way ANOVA with Sidak's multiple comparison. *N* = 6–14 mice/group derived from 2 independent experiments.

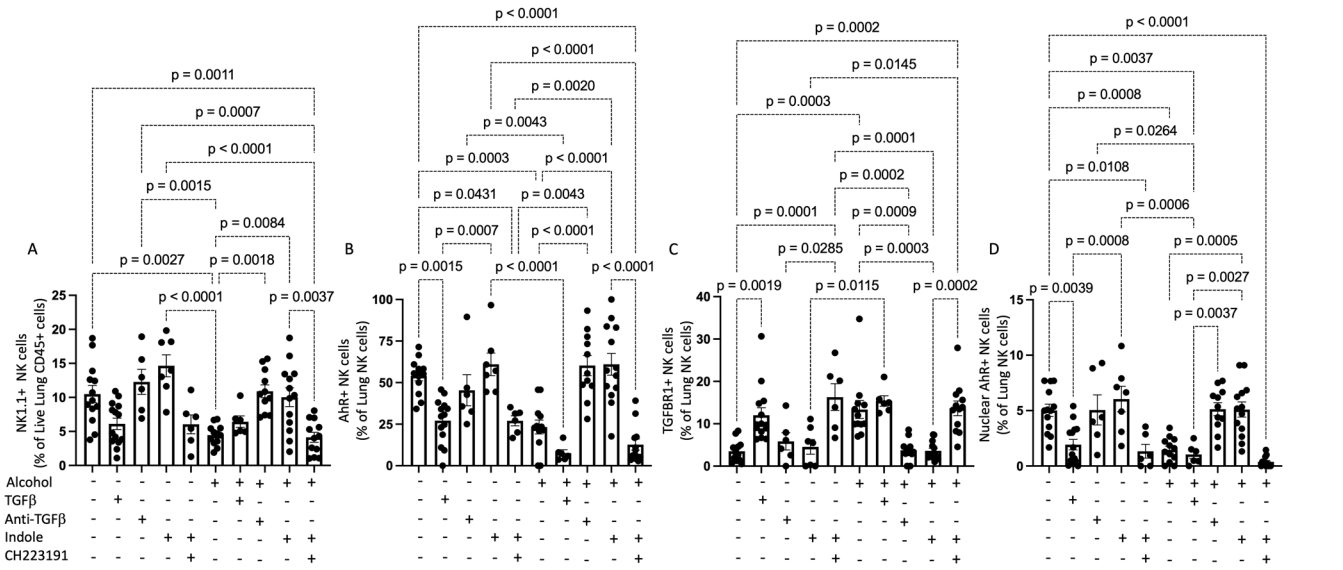

Fig. 5 | Alcohol alters the profile of pulmonary NK cells. Lungs were harvested from binge-on-chronic alcohol-fed mice with and without treatment post *K. pneumoniae* infection and the percentage and phenotype of pulmonary NK cells was assessed. The percentage of (**A**) NK1.1 cells, (**B**) AhR+ NK cells, (**C**) TGF-βR1 + NK cells, and (**D**) percentage of pulmonary NK cells with nuclear localization of AhR, was assessed using Anims FlowSight. *p* values are indicated by one-way ANOVA with Sidak's multiple comparisons. *N* = 6–14 mice/group derived from 2 independent experiments.

group is shown) were pooled to generate sufficient numbers of NK cells for ex-vivo testing. NK cells were isolated via negative selection and following purification a 90–95% pure population of NK cells was obtained (Fig. 9A). We first investigated the migratory capacity of the isolated NK cells using a Transwell migration assay. Strikingly, we observed two distinct migration response profiles to common NK cell chemokines. NK cells isolated from pair-fed mice, as well as alcohol-fed mice treated with indole, or anti-TGF-β1 monoclonal antibody readily migrated in response to CCL2 (Fig. 9C), CXCL12 (Fig. 9D) and CXC3CL1 (Fig. 9E) ($p < 0.0001$ in all cases) but were relatively non-responsive to CXCR3 signals including CXCL9, CXCL10, and CXCL11 (Fig. 9F). Conversely, we found that NK cells obtained from alcohol-fed mice or pair-fed mice treated with recombinant TGF-β1 readily

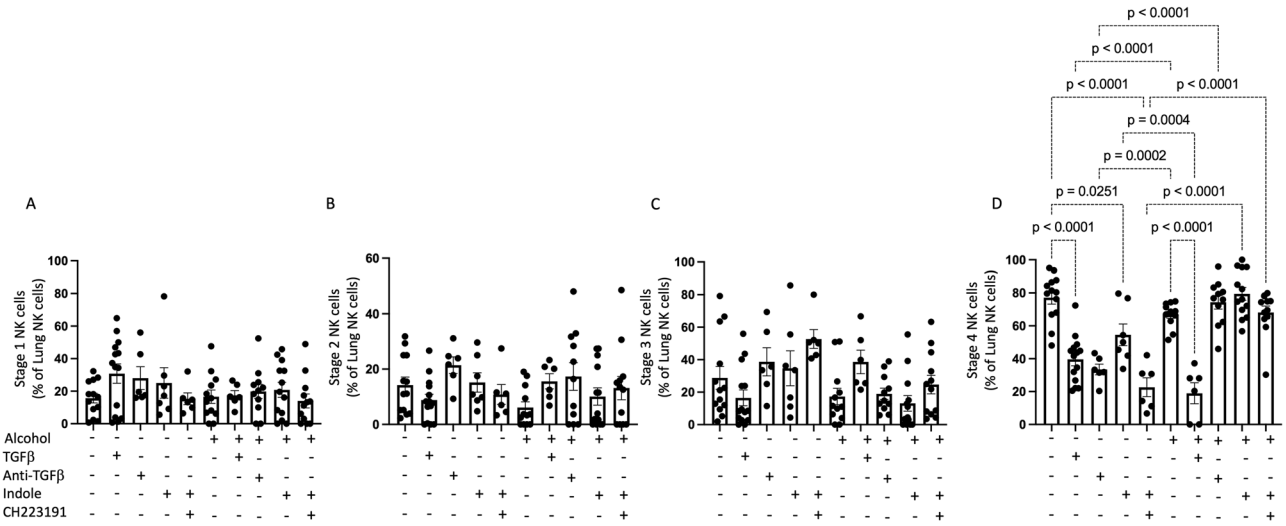

Fig. 6 | Alcohol decreases stage 4 mature pulmonary NK cells via alterations in AhR and TGF-β signaling. The proportion of pulmonary (**A**) stage I, (**B**) stage 2, (**C**) stage 3, and (**D**) stage 4 NK cells in binge-on-chronic alcohol mice treated with TGF-β1, anti-TGF-β1, indole, and CH223191. *p* values are indicated in the figure by one-way ANOVA with Sidak's multiple comparison. *N* = 6–14 mice/group derived from 2 independent experiments.

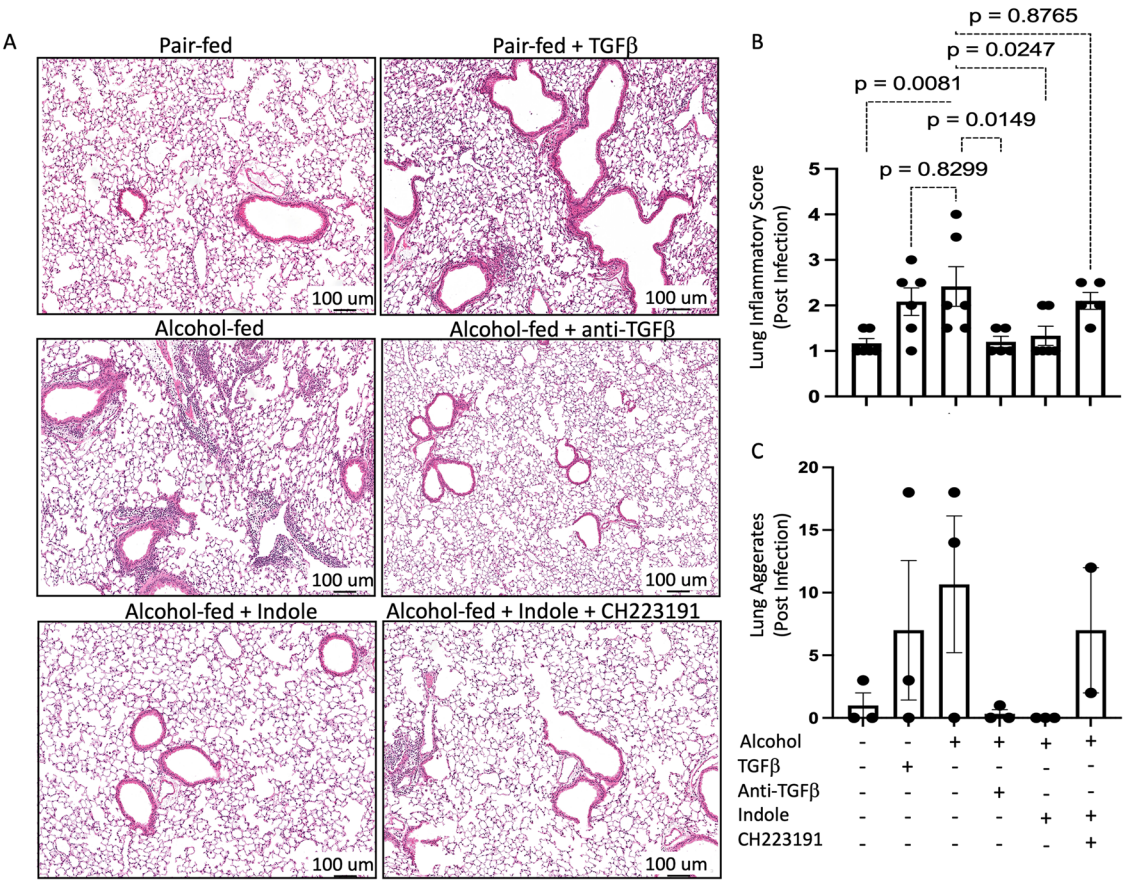

Fig. 7 | Pulmonary injury and inflammation following alcohol-associated bacterial pneumonia is mitigated by indole treatment. Alcohol-fed mice were infected with *K. pneumoniae*, and pulmonary damage was assessed 48 h. post-infection. **A** Representative pulmonary histology (20x magnification) of *K. pneumoniae* infected mice, **B** quantification of the lung inflammatory score, and (**C**) lung aggregates. *p* values are indicated in the figure by one-way ANOVA with Sidak's multiple comparison. *N* = 6 mice/group derived from 2 independent experiments.

migrated in response to CXCR3 signals including CXCL9, CXCL10, and CXCL11 (Fig. 9F), but were non-responsive to (Fig. 9C), CXCL12 (Fig. 9D) and CXC3CL1 (Fig. 9E) cytokines. Suggesting that alcohol use alters the NK cell chemoattractant response and migratory capacity.

In addition to migratory impairment, bactericidal capacity was substantially impaired in NK cells isolated from alcohol-fed mice or pair-fed mice treated with TGF-β1. NK cells isolated from pair-fed mice, as well as alcohol-fed mice treated with indole, or anti-TGF-β1 monoclonal

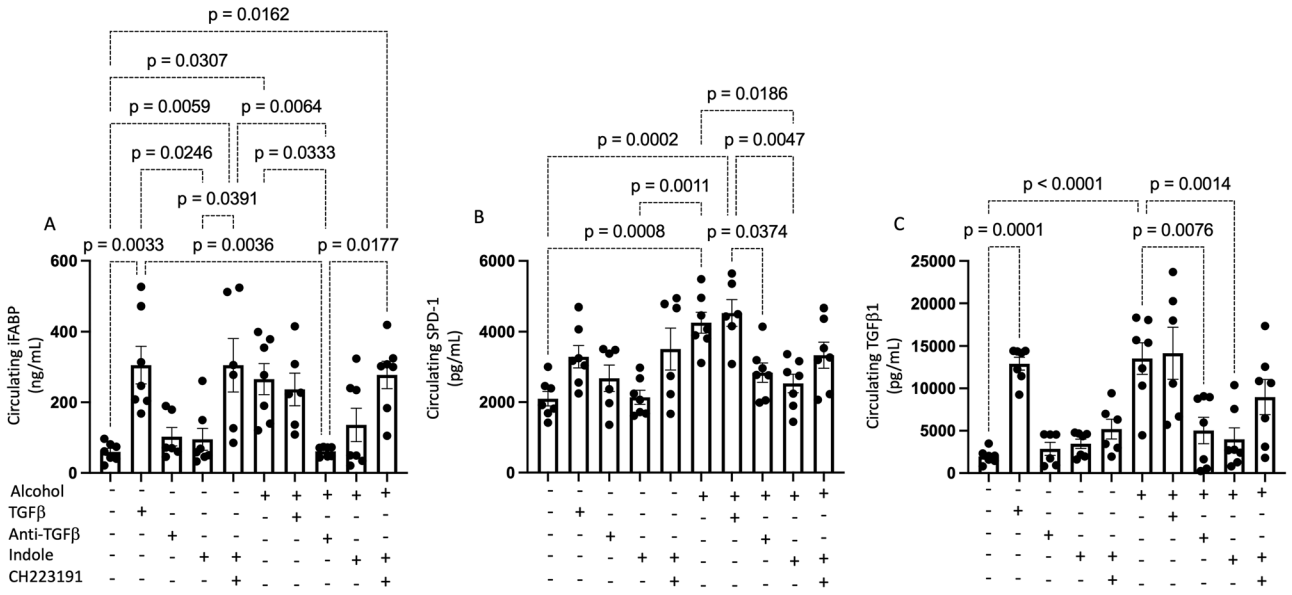

Fig. 8 | Alcohol increases epithelial barrier dysfunction and TGF-β1 levels. Alcohol-fed mice were infected with *K. pneumoniae*, and epithelial damage was assessed 48 h. post-infection. Circulating levels of (**A**) iFABP, (**B**) SDP-1, and (**C**) TGF-β1. *p* values are indicated in the figure by one-way ANOVA with Sidak's multiple comparison. *N* = 6–7 mice/group from 2 independent experiments.

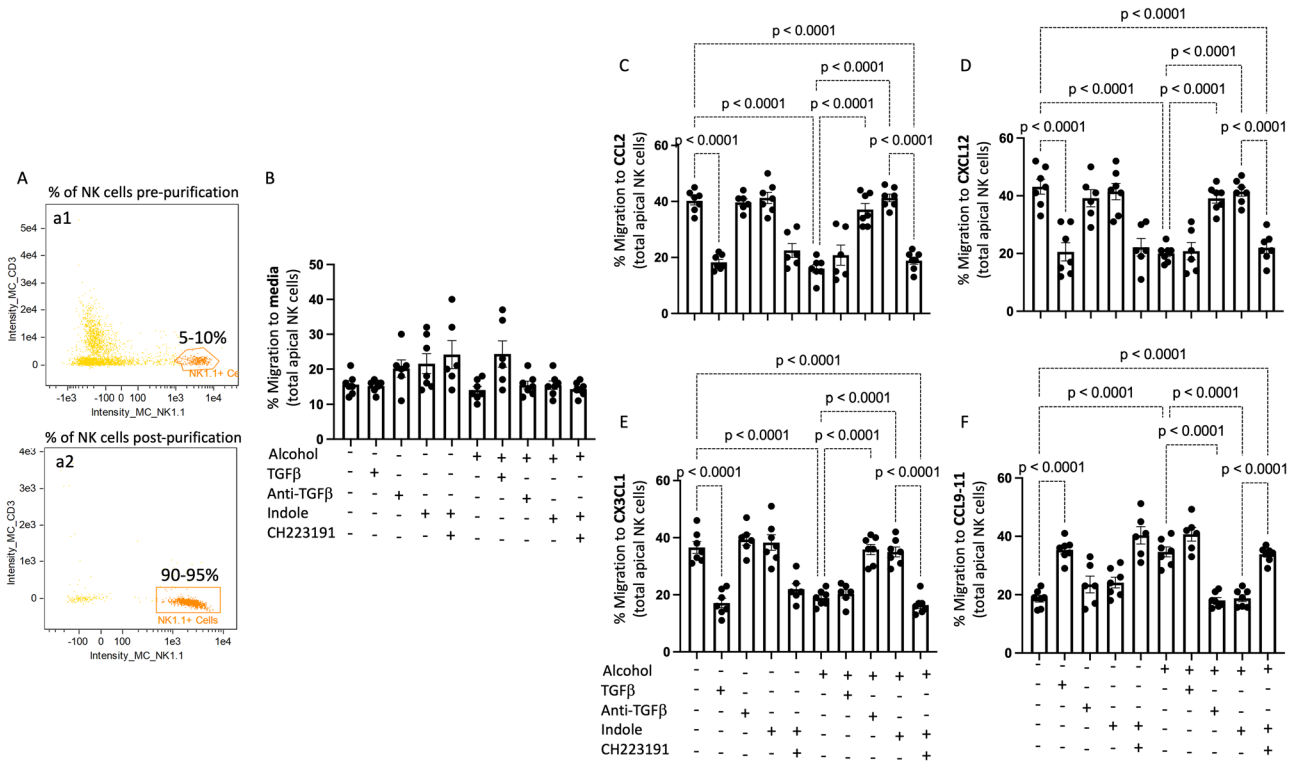

Fig. 9 | Alcohol dysregulates NK cell migration in response to chemokines. Mouse primary splenic NK cells were collected from alcohol-fed and treated mice and added to the apical side of a Transwell and migration in response to different chemokines was assessed following 5 h of incubation. **A** Confirmation of NK cell purification. (a1) Percentage of NK cells pre-isolation, and (a2) percentage of NK cells post-isolation. NK cell migration response profiles to (**B**) medial alone, (**C**) CCL2, (**D**) CXCL12, (**E**) CX3CL1, and (**F**) CCL9-11. Percent migration was calculated as the total number of viable NK cells in the bottom well divided by the total number of viable NK cells added to the Transwell insert. *p* values are indicated in the figure by one-way ANOVA with Sidak's multiple comparison. *N* = 6–7 wells of primary NK cells/group (12–14 mice/group, NK cells per 2 mice were pooled) derived from 2 independent experiments.

antibodies readily suppress bacterial viability to less than 25% of that observed for bacteria grown in media over the same timeframe (Fig. 10A). However, NK cells isolated from both alcohol and exogenous TGF-β1 treatment mice exhibit a near-complete abolishment of bacterial killing (Fig. 10A). We further validated these results with *Streptococcus pneumoniae*, a Gram-positive organism and leading cause of alcohol-associated bacterial pneumonia. NK cell-mediated killing of *S. pneumoniae* was significantly impaired by alcohol and TGF-β1 (Fig. 10B). In addition, we tested

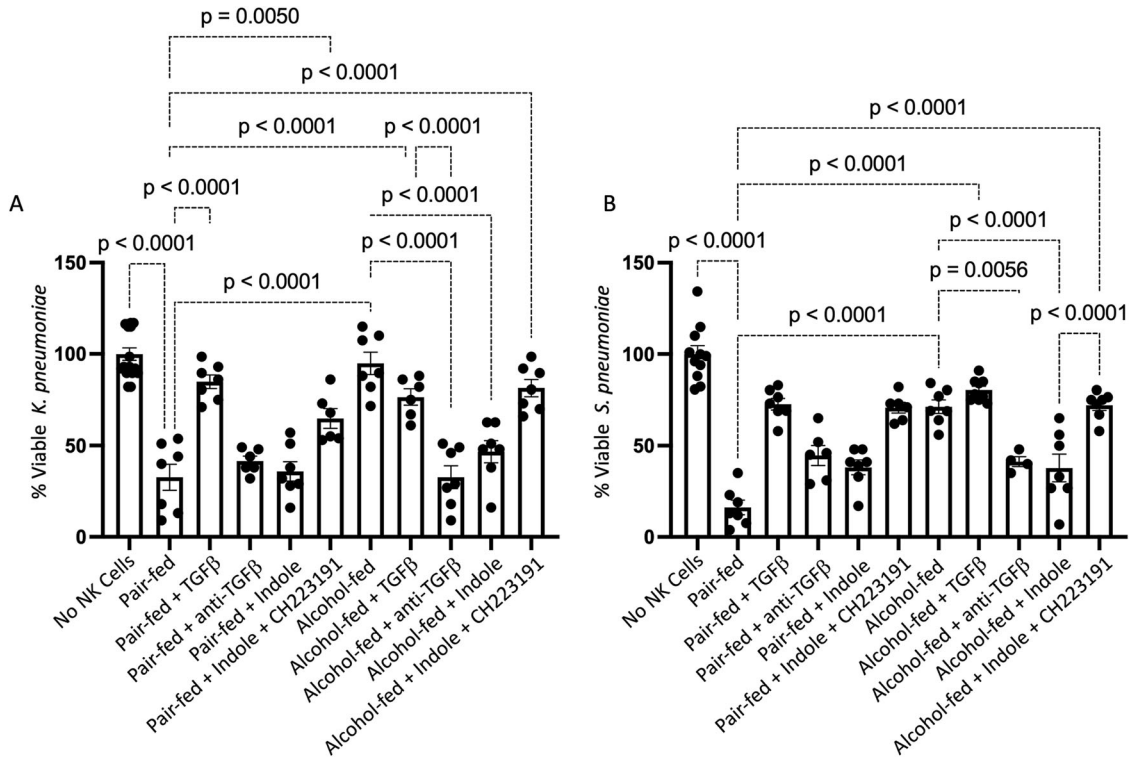

Fig. 10 | Alcohol dysregulates NK cell bactericidal capacity. Mouse primary splenic NK cells were collected from alcohol-fed and treated mice and co-cultured with bacteria for 3 h. **A** Percent viable *K. pneumoniae*, and (**B**) percent viable *S. pneumoniae* 3 h. post co-culture. Percent killing was calculated as the total number of viable bacteria post 3 h. incubation divided by the number of viable bacteria grown in OptiMEM without NK cells present. *p* values are indicated in the figure by one-way ANOVA with Sidak's multiple comparison. $N = 6–7$ wells of primary NK cells/group (12–14 mice/group, NK cells per 2 mice were pooled) derived from 2 independent experiments.

two human clinical isolates of *K. pneumoniae* for susceptibility to NK-mediated killing. Similar, to NK bactericidal capacity against the common ATCC 43816 strain of *K. pneumoniae*, we found that NK cells effectively kill both human isolates of *K. pneumoniae* (Fig. 11A). The loss of the NK bactericidal function appears to be partly attributable to dysfunction in granzyme-related pathways. Specifically, primary NK cells isolated from control animals were pretreated with various inhibitors prior to coculture with *K. pneumoniae*. NK cell treatment groups included: (1) Vehicle (0.1% DMSO), (2) Granzyme B inhibitor (10,000 ng/mL), (3) Concanamycin A (100 nM), (4) Granzyme B inhibitor and Concanamycin A, and (5) 100 μM 3,4-dichloroisocoumarin (DCI) for 1 h prior to co-culture with *K. pneumoniae*. Inhibition of Granzyme B or perforin did not significantly impair the bactericidal capacity of NK cells, however, the inhibition of total granzyme production with DCI greatly limited the bactericidal capacity of primary NK cells (Fig. 11B). Likewise, inhibition of Granzyme B or perforin did not significantly impair the bactericidal capacity of NK cells towards *S. pneumoniae* (Fig. 11C).

Treatment of human NK cells with exogenous alcohol or TGF-β significantly impairs NK cell function

We then tested the influence of exogenous alcohol and TGF-β1 on NK cell function using a human NK cell line (NK-92 cells). Specifically, NK-92 cells were pre-treated with 50 mM EtOH, 50 pg/mL of human TGF-β1, or with 20 μM indole and 50 mM EtOH for 24 h. Following incubation NK cell migratory capacity was assessed using the Transwell migration assay. NK-92 cells treated with either EtOH alone or with TGF-β1 failed to migrate in response to CCL2/CXCL12, compared to untreated NK-92 cells (Fig. 12). Further, alcohol-treated NK-92 cells which also were supplemented with exogenous indole had improved migratory capacity in response to CCL2/CXCL12, compared to alcohol-treated NK-92 cells (Fig. 12).

In addition to migratory impairment, bactericidal capacity was substantially impaired in NK-92 cells pretreated with alcohol. Specifically, NK-92 cells treated with EtOH for 24 h prior to co-culture with *Klebsiella* exhibited a dose-dependent decrease in bactericidal capacity, compared to untreated NK-92 cells (Fig. 13A). Additionally, NK-92 cells pre-treated with 50 mM EtOH or 50 pg/mL of human TGF-β1 exhibited decreased bactericidal capacity, while alcohol-treated NK-92 cells that were also supplemented with exogenous indole had improved NK cells bactericidal capacity (Fig. 13B). Finally, the effects of TGF-β1 suppression of NK-92 cells' bactericidal capacity was mitigated by exogenous indole treatment in a dose-dependent manner (Fig. 13B), but at a dose that was 100 times greater than that required to overcome the effects of alcohol alone. Like our mouse ex-vivo data, loss of the NK-92 bactericidal function was, in part, due to impaired granzyme production, as the inhibition of Granzyme B or perforin did not significantly impair the bactericidal capacity of NK-92 cells, but the inhibition of total granzyme activity significantly limited bactericidal capacity of NK-92 cells (Fig. 13C). Interestingly, in human NK cells, alpha-defensins may also play an important role in bactericidal activity against *K. pneumoniae*. Specifically, inhibition of alpha-defensin using a monoclonal antibody significantly limited the bactericidal capacity of NK-92 cells (Fig. 13C). In addition, we evaluated whether NK cell bacterial cell contact is required for bactericidal capacity. Using a Transwell model, we found that direct bacterial-NK cell contact was required for maximal bacterial killing, as there was no significant difference in the viability of *K. pneumoniae* when separated from NK cells via a 0.1 μm Transwell (Fig. 13D). We also tested two human clinical isolates of *K. pneumoniae* for susceptibility to NK (human NK-92 cells) mediated killing. Similar, to primary mouse NK cells, human NK-92 cells also killed both human clinical isolates of *K. pneumoniae* (Fig. 13E). In support of the in vitro NK cell assays, in vivo circulating levels of circulating alpha-defensin were suppressed in both alcohol and TGF-β1 treated groups (Fig. 14). In contrast, treatment of alcohol-fed mice

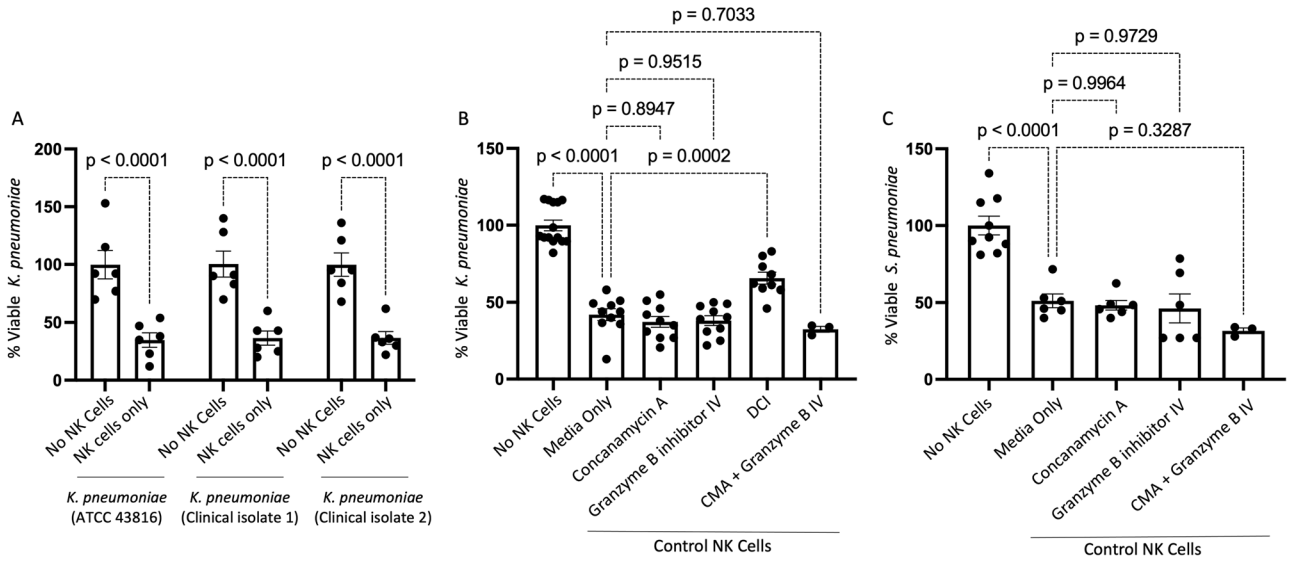

Fig. 11 | Mouse primary splenic NK cells were collected from wild-type mice and co-cultured with bacteria for 3 h. A Percent viable *K. pneumoniae* (ATCC 43816), *K. pneumoniae* (clinical isolate 1), *and K. pneumoniae* (clinical isolate 2). Primary control NK cells were pre-treated with various inhibitors prior to co-culturing with *K. pneumoniae or S. pneumoniae*. Percent viable (**B**) *K. pneumoniae* and (**C**) *S. pneumoniae* 3 h. post co-culture with inhibitor pre-treatment. *N* = 6–10 wells of primary NK cells derived from 2 independent experiments. *N* = 3 wells of primary NK cells for the combo treatment with CMA and Granzyme B IV inhibitors derived from 1 experiment.

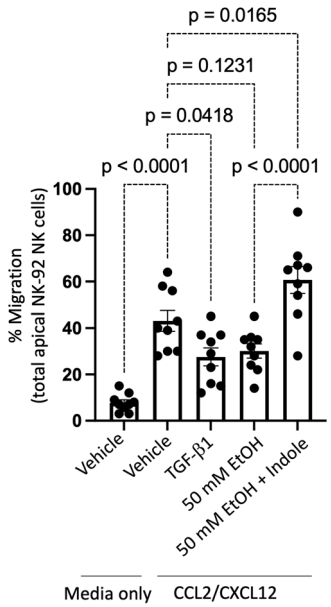

Fig. 12 | Alcohol dysregulates human NK cell migration. Human NK cells (NK-92 cell line) were treated with alcohol, indole, or recombinant TGF-β1, and NK cell migration in response to the CCL2/CXCL12 was assessed. *p* values are indicated in the figure by one-way ANOVA with Sidak's multiple comparison. *N* = 9 wells of NK-92 NK cells/group derived from 3 independent experiments.

with indole or anti-TGF-β1 restored circulating levels of alpha-defensin levels (Fig. 14). We predict that alpha-defensin is derived from the gut epithelium although this will require additional studies.

Discussion

Numerous preclinical and clinical studies have demonstrated the critical role intestinal microbiota play in regulating and facilitating pulmonary host defense against bacterial and viral infections[5,17–23]. Mice devoid of GI microbiota (germ-free mice) or mice with significantly depleted microbial communities (antibiotic-treated mice) are highly susceptible to pulmonary infection with various bacterial and viral pathogens, including *K. pneumoniae* and *S. pneumoniae*[17,18]. Several mechanistic pathways have been identified that regulate the gut-lung axis. Specifically, Nod-like receptor-stimulating bacteria present in the GI tract were shown to increase levels of interleukin-17A, which leads to the production of granulocyte-macrophage colony-stimulating factor and killing of bacterial pathogen by alveolar macrophages[18]. Enhanced susceptibility to *K. pneumoniae* in germ-free mice was also associated with increased levels of IL-10, decreased neutrophil pulmonary recruitment, and bacterial growth and dissemination[17]. However, the rigor of prior research linking alcohol-mediated gut dysbiosis to bacterial pneumonia is limited. In fact, to our knowledge, we are the only group to have investigated the role of alcohol-associated intestinal dysbiosis on pulmonary infections[5,24]. In addition, nothing is known about how alcohol might influence NK cell recruitment to the lungs.

NK cells have been classically viewed as crucial for innate defense against viruses and intracellular bacteria[25,26], however, emerging data indicate that NK cells also participate and are critical for optimal host defense against extracellular bacteria[27]. For example, it has been shown in mouse models that NK cells are required for optimal pulmonary host defense against *Pseudomonas aeruginosa*[28], and *Staphylococcus aureus*[29]. Similarly, NK cells are also required to combat infection of the GI tract with the extracellular bacterium *Citrobacter rodentium*[30]. In addition, lung NK cells promote host defense against respiratory infection by *K. pneumoniae* through the production of IL-22 and IFN-γ[13,31]. The mechanisms whereby NK cells protect against bacterial infections remain ill-defined, but the production of cytokines, such as TNF-α, IFN-γ, IL-22, and IL-10, leukocyte recruitment, macrophage activation, and direct bacterial killing are likely key mechanistic factors. More recently, NK cells have been shown to play a critical role in the killing of extracellular *P. aeruginosa*[32]. Specifically, NK cells killed extracellular *P. aeruginosa* via contact-dependent production of multiple granzymes, namely granzyme B and H[32]. Like our data, perforin, granzyme B, or granulysin alone were sufficient for NK cell-mediated killing of *P. aeruginosa*[32]. Together this data supports the fact that NK cells also play a critical role in host defense against extracellular pathogens. Alcohol misuse is known to quantitatively and qualitatively alter NK cell function[33]. Specifically, alcohol reduces peripheral NK cell numbers, increases the number of IFN-γ producing NK cells, and compromises NK cell cytolytic activity by inhibiting the production of perforin, granzyme A, and granzyme B[34–36].

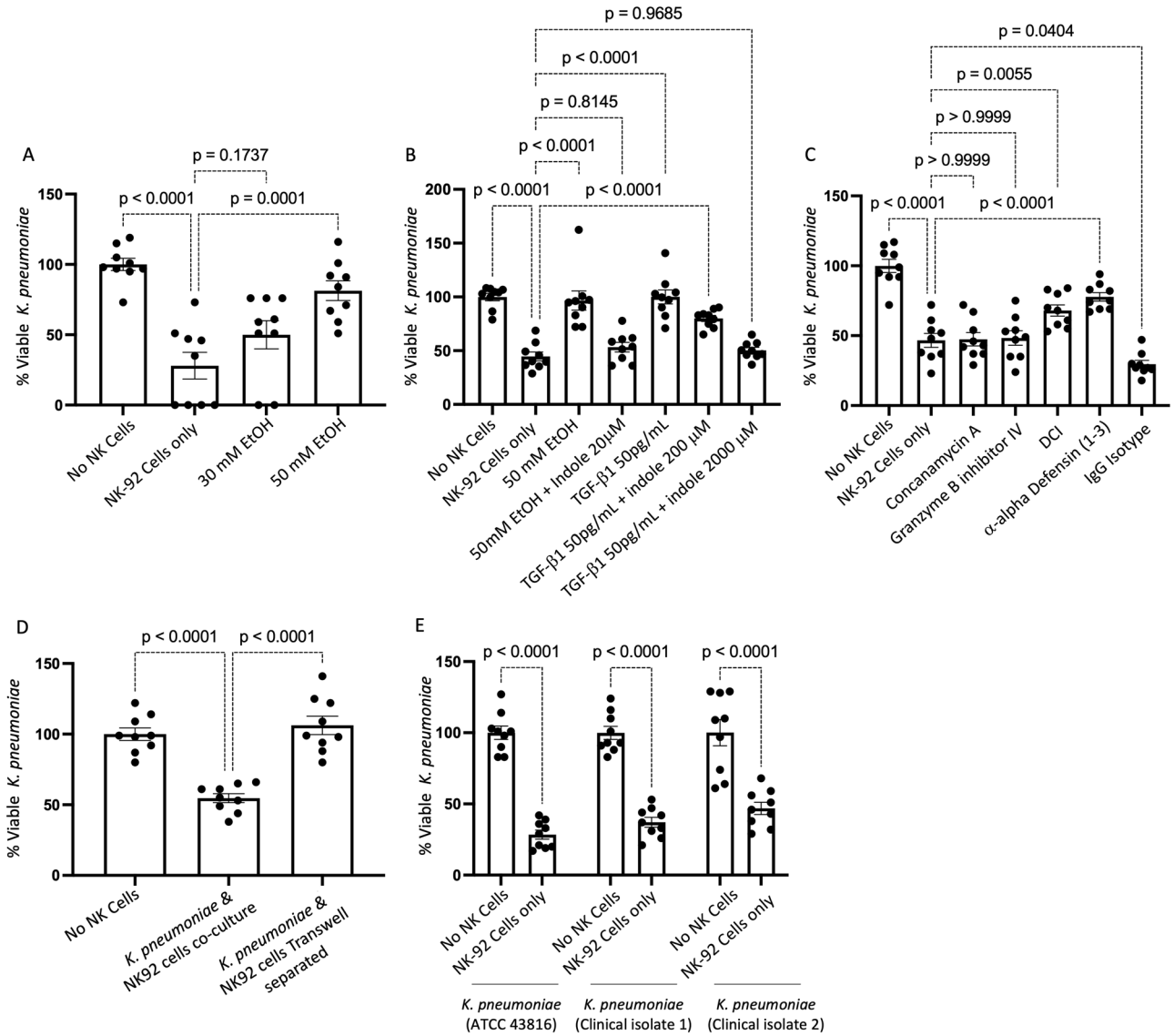

Fig. 13 | Alcohol dysregulates human NK cell bactericidal capacity. Human NK cells (NK-92 cell line) were treated with alcohol, indole, or recombinant TGF-β1, and NK cell bactericidal capacity was assessed. **A**–**D** Percent viable *K. pneumoniae* 3 h. post co-culture with NK cells pre-treated with different compounds/inhibitors. **A** Ethanol dose-dependent inhibition of bactericidal capacity. **B** Inhibition of bactericidal capacity via TGF-β1 and rescue of alcohol-mediated and TGF-β1-mediated inhibition via indole. **C** NK cell bactericidal capacity is mediated via alpha-defensin and total granzyme production. **D** NK cell bactericidal capacity is contact-dependent. **E** NK cell bactericidal capacity against clinical isolates. *p* values are indicated in the figure by one-way ANOVA with Sidak's multiple comparison. *N* = 9 wells of NK-92 NK cells/group derived from 3 independent experiments.

Recently, AhR signaling has emerged as a potential link between the intestinal microbiota and the host immune system, especially regarding host defense against pathogenic insult. For example, the AhR-dependent expression of IL-22 is critical for host defense against *Candida albicans*[12]. Additionally, mice treated with antibiotics exhibited marked impairments in lung immunity to *P. aeruginosa* via decreased AhR expression in the intestinal tract and reduced peroxynitrite production by AMs. Importantly, augmentation of AhR signaling by tryptophan supplementation (catabolized by the microbiota into AhR ligands) decreases *P. aeruginosa* bacterial counts in the lung and increases intestinal ROS production, as well as the phagocytic activity of AMs[37]. AhR signaling was first demonstrated to be important for the development and differentiation of regulatory and Th17 T-cells[38]. Since then, AhR expression has been reported in specialized innate lymphoid cells[39], as well as in a number of other hematopoietic populations. Recently, NK cells were found to express AhR upon cytokine stimulation[40–42]. Interestingly, determinants of AhR activity, including AhR ligands found in the diet, were found to modulate the antitumor effector functions of NK cells[41]. Similarly, the activity of NK cells is strongly affected by TGF-β. Specifically, TGF-β is known to; (1) negatively regulate IFN-γ production[43], (2) decrease the surface level of the activating receptors NKG2D and NKp30[44], (3) decrease cytotoxicity[45], and (4) decrease the antitumor function of NK cells[45]. TGF-β is also known to alter the surface expression of the chemokine receptors CXCR3, CXCR4, and CX3CR1, possibly altering NK cell migration and recruitment[44].

We propose that indole and TGF-β1 exert counter-regulatory effects through differential genetic expression regulated by AhR and SMAD2/3, respectively. The experiments above establish that AhR and TGF-β1 interplay is relevant for a variety of immunological processes including circulating levels of alpha-defensins, NK cellular migration, and NK cytotoxicity, as well as epithelial barrier function. In addition, our data suggests that alcohol may likewise interfere with NK cell maturation through changes in AhR and SMAD2/3 signaling, although lineage-tracking experiments are

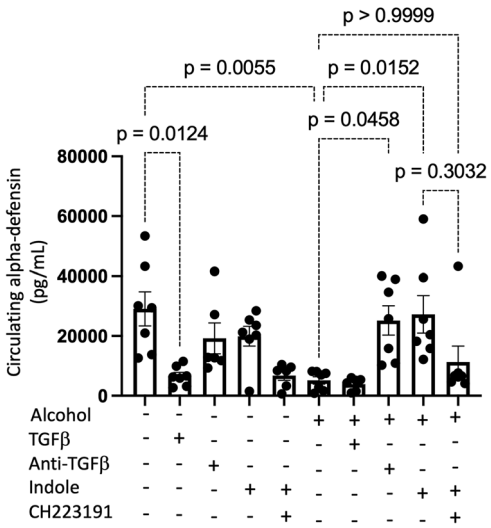

Fig. 14 | Alcohol decreases circulating alpha-defensin 1 levels. Alcohol-fed mice with and without treatments were infected with *K. pneumoniae* and serum was collected 48 h. post infection. Circulating levels of alpha-defensin 1 48 h. post infection; *p* values are indicated in the figure by one-way ANOVA with Sidak's multiple comparison. $N = 6–7$ mice/group from 2 independent experiments.

needed to validate these observations. Exposure to alcohol, through TGF-β signaling, alters the functional effectiveness and phenotypic characteristics of pulmonary NK cells. However, whether this represents a change in gene expression of circulating pools of NK cells or in the maturation of NK cells from stage 1 to stage 4 cells, or both, is unknown. We currently favor the latter explanation and contend that SMAD2/3 and AhR signaling are opposing forces that control whether NK cells shift from a "normal" response profile to an "alcohol-associated" response profile. More precisely, following pulmonary infection, NK cells with a "normal" profile robustly respond to chemokines, such as CCL2, CXCL12, and CXC3L1, while the phenotype of alcohol-exposed NK cells inverts to respond preferentially to CXCL9-11 chemokines.

There are several limitations to the current study, which require additional investigation. We also observed the depletion of NKT cells in using the NK1.1 depletion approach, as such it is necessary to further evaluate the contribution of NKT cells in pulmonary host defense. However, our in vitro data with NK cells and indole supplementation supports the role of NK cells in host defense against alcohol-associated bacterial infections. We also only utilized female mice for these experiments, knowing that gender differences have been observed in other alcohol-associated pathologies, future studies will need to evaluate male, as well as female mice. Also, while our ex-vivo data suggest that NK cells may shift from a "normal" chemokine receptor profile to an "alcohol-associated" chemokine receptor profile we cannot rule out that in vivo trafficking effects are due to local production of chemokines, i.e., alcohol-associated lungs produce significantly less CCL2. The effects of TGF-β and alcohol seen in our animal models suggest that either ligand or receptor levels or both may underly the detrimental effects seen in vivo, however further studies are needed to evaluate whether ligand or receptor levels drive the observed effects. The role of cellular proliferation of NK cells locally and in other distal tissues likewise needs further evaluation. While our data supports changes in migratory capacity, we cannot rule out alterations in proliferation capacity. Finally, the sources of TGF-β or alpha-defensin in the host are unknown and may change in relation to barrier function independent of NK cells.

This study focused on the relationship between alcohol, TGF-β and AhR signaling in NK cells, and host defense against bacterial pneumonia. Together this data suggests that alcohol causes disruption of NK cell-specific TGF-β and AhR signaling leading to decreased pulmonary recruitment and cytolytic activity thereby increasing susceptibility to alcohol-associated bacterial pneumonia. Understanding the role of intestinal dysbiosis and TGF-β/AhR signaling pathways in the context of alcohol-associated pneumonia may foster novel prophylactic strategies (i.e., indole treatment) for the prevention of alcohol-associated pneumonia in high-risk individuals, which could be especially impactful for individuals with limited resources and access to alcohol treatment centers.

Methods

Mice

Female 10–12-week-old C57BL/6 mice were obtained from Charles Rivers Breeding Laboratories (Wilmington, MA) and maintained in Comparative Medicine at UNMC. Food and water were provided *ad libitum*. All mice were housed in an SPF environment under standard social housing conditions with appropriate environmental enrichment. All protocols used in these studies were approved by the Institutional Animal Care and Use Committee of UNMC (IACUC# 19-120-11-EP). This research protocol is in accordance with the NIH and Office of Laboratory Animal Welfare (OLAW) guidelines.

Alcohol feeding model

We utilized a binge-on-chronic alcohol feeding model as we have previously published[5]. All animals were acclimated to a liquid diet for 5 days using Lieber-DeCarli '82 Shake and Pour (Bioserv, Flemington, NJ. Cat. No. F1259). Groups of mice ($n = 3$ per cage) were randomized into ethanol-fed (Bioserv. Cat. No. F1258), ethanol-fed plus treatment, or pair-fed groups. Pair-fed mice were maintained on a control-liquid diet adjusted daily according to the consumption of ethanol-fed mice. Mice were administered 4 g kg^{-1} (31.5% vol/vol) ethanol by gavage following 5 and 10 days of alcohol-feeding. Pair-fed control mice were gavaged with 7 g kg^{-1} (45% wt/vol) maltose dextrin on days 5 and 10 of control-diet feeding.

Exogenous treatments (Indole, CH223191, anti-TGF-β1, and TGF-β1 treatment)

Mice were treated by oral gavage daily throughout the course of the experiments with indole or CH-223191. Mice received indole by gavage (20 mg/kg/dose indole: Sigma Aldrich, St. Louis, MO. Cat. No. BP0057) dissolved in sterile water warmed to 55 °C. Mice received CH-223191 by gavage (10 mg/kg/dose or ~200 µL of 3 mM CH-223191: MedChemExpress, Monmouth Junction, NJ. Cat. No. HY-12684) dissolved in sterile corn oil. Mice were treated via IP injection with recombinant TGF-β1 or anti-TGF-β1 every 3 days with the first dose coinciding with the initiation of alcohol-feeding. Mice were treated with mouse InVivoPlus anti-TGF-β1 monoclonal antibody (clone: 1D11.16.8) by IP injection (10 mg/kg/dose, of mouse anti-TGF-β1; BioXCell, Lebanon, NH. Cat. No. BP0057). Mice were treated with mouse recombinant TGF-β1 by IP injection (0.5 µg/g/dose of rTGF-β1: MedChemExpress. Cat. No. HY-P7117). All mice not receiving treatment via oral gavage were also gavaged daily with vehicle (PBS). Similarly, animals not receiving IP treatments were IP injected with a mouse IgG1 isotype control antibody (clone MOPC-21) in PBS (10 mg/kg/dose, of mouse IgG1 isotype control: BioXCell. Cat. No. BE0083).

NK cell depletion

Mice were depleted of NK cells via IP injection with anti-NK1.1 monoclonal antibody every 3 days with the first dose coinciding with the initiation of alcohol-feeding. Mice were treated with InVivoPlus mouse anti-NK1.1 (clone: PK136) monoclonal antibody by IP injection (10 mg/kg/dose, of mouse anti-NK1.1; BioXCell. Cat. No. BP0036). All control mice were given IP injected with a mouse IgG1 isotype control antibody (clone MOPC-21) in PBS (10 mg/kg/dose, of mouse IgG1 isotype control: BioXCell. Cat. No. BE0083).

Klebsiella pneumoniae infection

Klebsiella pneumoniae infections and burden assessments were performed using standard methods[5]. Briefly, *K. pneumoniae* (Strain 43816, serotype 2; American Type Culture Collection [ATCC], Manassas, VA. Cat. No. 43816)

was grown in 100 mL tryptic soy broth (Becton Dickinson, Franklin Lakes, NJ) in a shaking incubator at 37 °C for 18 h. Bacteria were then pelleted and resuspended in PBS at an estimated concentration of 1×10^3 colony-forming units (CFU)/mL. Mice were then infected with 100 µl of inoculum (1×10^2 CFU) via oropharyngeal aspiration. Mice were sacrificed 48 h post-infection, and the pulmonary and splenic burden was determined via serial dilution and plating onto HiCrome Klebsiella Selective Agar plates.

Lung histology

Whole lungs were inflated with 10% formalin (ThermoFisher Scientific) to maintain pulmonary structure. The UNMC Tissue Sciences Core Facility processed all the lungs. Specifically, lungs were paraffin-embedded and 4–5 µm sectioned were mounted on glass slides and stained with hematoxylin and eosin. The Leica Aperio CS2 (Leica Biosystems, Deer Park, IL) imaging system and the Leica ImageScope software were used to obtain all images (20x). Lung inflammation was scored by a blinded pathologist using a previously published scoring system[46,47].

Serum analysis

Serum was collected from all mice at sacrifice using BD serum separator tubes (BD Biosciences, San Jose, CA). Mouse serum levels of SPD-1 were detected via the Mouse SP-D Quantikine ELISA Kit (Novus Biologicals, Centennial, CO. Cat. No. MSFPD0). Mouse serum levels of IFABP were detected using the Mouse FABP2/I-FABP ELISA Kit (Novus Biologicals. Cat. No. NBP2-82214). Mouse alpha-defensin levels were detected using the Mouse Defensin Alpha 1ELISA Kit (LS Bio, Shirley, MA. Cat. No. LS-F6926-1). Mouse TGF-β1 levels were determined using the Mouse TGF-beta 1 DuoSet ELISA (R&D Systems, Minneapolis, MN. Cat. No. DY1679). Mouse IL-22 levels were determined using the Mouse/Rat IL-22 Quantikine ELISA Kit (R&D Systems. Cat. No. M2200). ELISA Kits were run according to the manufacturer's specifications.

Flow cytometry

Lung immune cells were collected for flow cytometry analysis[5]. The lung tissue of each animal was collected into C-tubes and immune cells were isolated using the mouse Lung Dissociation Kit (Miltenyi Biotec, Auburn, CA. Cat. No. 130-095-927) according to the manufacturer's specifications. Lung samples were homogenized using gentleMACS™ Octo Dissociator (Miltenyi Biotec). Following isolation, any remaining red blood cells (RBCs) were lysed using RBC lysis buffer (BioLegend, San Diego, CA. Cat. No. 420301) prior to staining. After washing with PBS, viable cells were counted on a hemocytometer using the trypan blue–exclusion method. One million viable cells were then used for staining. Lung immune cells were pretreated with TruStain FcX Anti-mouse CD16/32 antibody (BioLegend. 2 µL per test, Cat. No. 101320) and then stained with LIVE/DEAD™ Fixable Violet Dead Cell Stain Kit (ThermoFisher Scientific, Waltham, MA. 1 µL/test, Cat. No. L34955, Invitrogen, Eugene, OR) followed by surface staining with antibodies specific for murine CD45 Brilliant Violet 510 (BioLegend. 0.50 µg per test, Cat. No. 103137), CD3 PE-Cyanine5 (BioLegend. 0.30 µg per test, Cat. No. 100274), NK1.1 PE-eFluor™ 610 (ThermoFisher Scientific. 0.50 µg per test, Cat. No. 61-5941-82), CD11b APC-Cyanine7 (BioLegend. 0.60 µg per test, Cat. No. 101226), CD27 APC (BioLegend. 0.20 µg per test, Cat. No. 124212), TGF-βR1 PE (ThermoFisher Scientific. 10 µL per test, Cat. No. FAB5871P100). Cells were then fixed and permeabilized using the True-Nuclear™ Transcription Factor Buffer Set, according to manufacturers' specifications (BioLegend. Cat. No. 424401). Cells were then stained for the intracellular markers AhR Alexa Fluor® 488 (BD Biosciences, Franklin Lakes, NJ. 0.20 µg per test, Cat. No. 565788), and the nuclear stain DRAQ5 (BD Biosciences. 1.0 µL of a 1/1000 dilution of the stock per test, Cat. No. 564903). All samples were stained in the presence of BD Horizon™ Brilliant Stain Buffer (BD Biosciences. 50 µL per test, Cat. No. 100274). For all experiments, cells were acquired using an Amnis® FlowSight® Imaging Flow Cytometer (Millipore Sigma, Burlington, MA). Cells were analyzed using the IDEAS® Software package (Millipore Sigma).

NK cell isolation

The spleen was harvested at sacrifice, resuspended in PBS, and homogenized using gentleMACS™ Octo Dissociator (Miltenyi Biotec). Whole blood was collected using BD Microtainer® Blood Collection Tubes with K2EDTA (BD Biosciences). Splenic homogenates and whole blood were then combined and red blood cells (RBCs) were lysed using RBC lysis buffer (BioLegend, Cat. No. 420301). NK cells were then isolated using the NK Cell Isolation Kit, mouse (Miltenyi Biotec, Cat. No. 130-115-818), according to manufacturers' recommendations. Isolated NK cells were then cultured in NK MACS Medium (Miltenyi Biotec, Cat. No. 130-114-429) containing 5% Horse Serum (ThermoFisher. Cat. No. 16050130), 100 U/mL and 100 µg/mL of penicillin/streptomycin (Sigma. Cat. No. P4333-100ML), and 500 IU/mL of mouse IL-2 (ThermoFisher. Cat. No. PMC0025) for 24 h at 37 °C with 5% CO_2. Following 24 h of incubation NK cell migration and bactericidal activity were assessed, described below.

Human NK cells

Human NK-92 cells were obtained from (American Type Culture Collection. Cat. No. CRL-2407). NK-92 cells were cultured in NK MACS Medium (Miltenyi Biotec, Cat. No. 130-114-429) containing 5% Horse Serum (ThermoFisher. Cat. No. 16050130), 100 U/mL and 100 ug/mL of penicillin/streptomycin (Sigma. Cat. No. P4333-100ML), and 500 IU/mL of human IL-2 (ThermoFisher. Cat. No. PMC0025). NK-92 cells were incubated at 37 °C with 5% CO_2. Cells were maintained at a density of ~2×10^5 viable cells/mL and subcultured every 2–3 days depending on density.

NK cell migration assay

Primary mouse NK cells. NK cell migration was assessed using Corning® Transwell® polycarbonate membrane cell culture inserts (Sigma, Cat. No. CLS3421-48EA). The number of viable Primary NK cells was determined following 24 h of culture via trypan blue staining. NK cells were centrifuged at 300 × ~*g* for 10 min and resuspended in fresh Opti-MEM at a density of 1×10^7 viable cells/mL, and 100 µL of the NK cell suspension was added to the Transwell insert. 600 µL OptiMEM only, or OptiMEM containing 50 ng/mL of CCL2 (Sigma. Cat. No. 45-SRP3215-10UG), 100 ng/mL of CXCL12 (R&D Systems, Cat. No. 460-SD-050), 100 ng/mL of CXCL9 (R&D Systems, Cat. No. 492-MM-010), 100 ng/mL CXCL10 (R&D Systems, Cat. No. 466-CR-010), 100 ng/mL CXCL11 (R&D Systems, Cat. No. 572-MC-025), 300 ng/mL CX3CL1 (R&D Systems, Cat. No. 472-FF-025) was added to the bottom of the of the Transwell. Migration was then assessed by determining the number of viable cells in the bottom culture well 5 h post incubation. Percent migration was calculated as the total number of viable NK cells in the bottom well divided by the total number of viable NK cells added to the Transwell insert. No differences were seen in cell viability between groups post-migration assay.

Human NK-92 cells. NK-92 cell migration was assessed as described for primary mouse NK cells, with the following modifications. NK-92 cells were first pretreated with 50 pg/mL of human recombinant TGF-β1 (R&D Systems, Cat. No. 7754-BH-025/CF), 50 mM EtOH, or 50 mM EtOH with 20 µM indole for 24 h. Following pre-treatment NK cells were centrifuged at 300 × ~*g* for 10 min and resuspended in fresh OptiMEM at a density of 1×10^7 viable cells/mL, and 100 µL of the NK cell suspension was added to the Transwell insert. 600 µL OptiMEM only, or OptiMEM containing 50 ng/mL of CCL2 (R&D Systems. Cat. No. 279-MC-050/CF) and 100 ng/mL of CXCL12 (R&D Systems, Cat. No. 350-NS-050/CF) was added to the bottom of the Transwell. Migration was then assessed by determining the number of viable cells in the bottom culture well 5 h post incubation. No differences were seen in cell viability between groups post-migration assay.

NK cell bactericidal activity

Primary mouse NK cells. NK cell bactericidal capacity was assessed by co-culturing NK cells with *Klebsiella pneumoniae* (ATCC, Cat. No.

43816) or *Streptococcus pneumoniae* (Strain TIGR4 [JNR.7/87], serotype 4; ATCC, Cat. No. BAA0334). *Klebsiella pneumoniae* de-identified clinical isolates were obtained from the Nebraska Medicine Clinical Microbiology Laboratory. Primary NK cells isolated from each of the mouse treatment groups were centrifuged at 300 × ~*g* for 10 min and resuspended in fresh OptiMEM at a density of 1×10^6 viable cells/mL. 100 µL of the primary NK cells were added to 900 µL (1×10^5 cells/well) of OptiMEM. In addition, a separate set of primary NK cells isolated from control mice was added to OptiMEM containing 10,000 ng/mL of Granzyme B inhibitor (Sigma, Cat. No. 368056), 100 nM of Concanamycin A (Sigma, Cat. No. C9705), or 100 µM of the total granzyme inhibitor 3,4-dichloroisocoumarin (DCI; MilliporeSigma, Cat No. 287815-10MG) for 1 h prior to co-culture with bacteria. *K. pneumoniae* was grown in 100 mL tryptic soy broth (BD Biosciences) in a shaking incubator at 37 °C for 18 h. Bacteria were then pelleted and resuspended in PBS at an estimated concentration of 1×10^7 colony-forming units (CFU)/mL. *S. pneumoniae* was grown in 100 mL Todd Hewitt Broth (BD Biosciences) at 37 °C in 5% CO_2 for 6 h. Bacteria were then pelleted and resuspended in PBS at a concentration of 1×10^7 CFU/mL. Bactericidal activity was then assessed by adding 100 µL (MOI of 10) of either *K. pneumoniae* or *S. pneumoniae* to the wells containing NK cells and incubated for 3 h. The number of viable *K. pneumoniae* and *S. pneumoniae* 3 h post-infection was determined via serial dilution and plating onto BD BBL™ Trypticase™ Soy Agar (TSA II™) with sheep blood (BD Biosciences). Contact-dependent bactericidal capacity was assessed using Transwells. Specifically, *K. pneumoniae* was prepared as described above and added to the top well of the 0.1 µM Transwells, or in the bottom well with/without NK-92 cells at an MOI 0 f 10 and incubated for 3 h. The number of viable *K. pneumoniae* 3 h post-infection was determined via serial dilution. Percent killing was calculated as the total number of viable bacteria post 3 h. incubation divided by the number of viable bacteria grown in OptiMEM without NK cells present.

Human NK-92 cells. NK-92 cell bactericidal activity was assessed as described for primary mouse NK cells, with the following modifications. NK-92 cells were first pretreated with 50 pg/mL of human recombinant TGF-β1 (R&D Systems, Cat. No. 7754-BH-025/CF), 30 mM EtOH, 50 mM EtOH, 50 mM EtOH with 20 µM indole, and 50 pg/mL of human recombinant TGF-β1 in the presence of 200, and 2000 µM indole for 24 h. In addition, separate set experiments with NK-92 cells, cells were pretreated with 10,000 ng/mL of Granzyme B inhibitor (Sigma, Cat. No. 368056), 100 nM of Concanamycin A (Sigma, Cat. No. C9705), 100 µM of the total granzyme inhibitor DCI, 1 µg/mL of anti-human DEFA1-3 (Alpha Diagnostic International, San Antonio, TX. Cat. No. HDEFA11-A), or 1 µg/mL mouse IgG1 isotype control (BioXCell. Cat. No. BE0083) for 1 h prior to co-culture with bacteria. Bactericidal activity was then assessed as described above.

Statistics and reproducibility

Statistical analyses were performed using GraphPad Prism 10 (La Jolla, CA). Results are shown as the mean ± standard error of the mean. A $p < 0.05$ was deemed significant. Sample size and number of replicates are indicated in each respective figure legend. Statistical significance was assessed using a Mann–Whitney test for comparisons between two groups and a one-way analysis of variance (ANOVA) with Sidak's multiple comparison test for comparisons between three or more groups.

Reporting summary

Further information on research design is available in the Nature Research Reporting Summary linked to this article.

Data availability

All the data that support the findings of this study are available within the paper and are available at https://doi.org/10.6084/m9.figshare.24050628.v1.

Received: 5 September 2023; Accepted: 25 August 2024;
Published online: 03 September 2024

References

1. Simet, S. M. & Sisson, J. H. Alcohol's effects on lung health and immunity. *Alcohol Res.* **37**, 199–208 (2015).
2. Happel, K. I. & Nelson, S. Alcohol, immunosuppression, and the lung. *Proc. Am. Thorac. Soc.* **2**, 428–432 (2005).
3. Jong, G. M., Hsiue, T. R., Chen, C. R., Chang, H. Y. & Chen, C. W. Rapidly fatal outcome of bacteremic Klebsiella pneumoniae pneumonia in alcoholics. *Chest* **107**, 214–217 (1995).
4. Sisson, J. H. Alcohol and airways function in health and disease. *Alcohol* **41**, 293–307 (2007).
5. Samuelson, D. R. et al. Alcohol-associated intestinal dysbiosis impairs pulmonary host defense against Klebsiella pneumoniae. *PLoS Pathog.* **13**, e1006426 (2017).
6. Samuelson, D. R. et al. Pulmonary immune cell trafficking promotes host defense against alcohol-associated Klebsiella pneumonia. *Commun. Biol.* **4**, 997 (2021).
7. Sin, D. D., Leung, R., Gan, W. Q. & Man, S. P. Circulating surfactant protein D as a potential lung-specific biomarker of health outcomes in COPD: a pilot study. *BMC Pulm. Med.* **7**, 13 (2007).
8. Kano, H. et al. Prediction of reversibility of intestinal mucosal damage after ischemia-reperfusion injury by plasma intestinal fatty acid-binding protein levels in pigs. *Perfusion* **30**, 617–625 (2015).
9. Schurink, M. et al. Intestinal fatty acid-binding protein as a diagnostic marker for complicated and uncomplicated necrotizing enterocolitis: a prospective cohort study. *PLoS One* **10**, e0121336 (2015).
10. Morris, M. A. & Ley, K. Trafficking of natural killer cells. *Curr. Mol. Med.* **4**, 431–438 (2004).
11. Kim, Y. K. et al. Increased transforming growth factor-beta1 in alcohol dependence. *J. Korean Med. Sci.* **24**, 941–944 (2009).
12. Zelante, T. et al. Tryptophan catabolites from microbiota engage aryl hydrocarbon receptor and balance mucosal reactivity via interleukin-22. *Immunity* **39**, 372–385 (2013).
13. Xu, X. et al. Conventional NK cells can produce IL-22 and promote host defense in Klebsiella pneumoniae pneumonia. *J. Immunol.* **192**, 1778–1786 (2014).
14. Yang, W. et al. Intestinal microbiota-derived short-chain fatty acids regulation of immune cell IL-22 production and gut immunity. *Nat. Commun.* **11**, 4457 (2020).
15. Zou, J. et al. Inulin fermentable fiber ameliorates type I diabetes via IL22 and short-chain fatty acids in experimental models. *Cell Mol. Gastroenterol. Hepatol.* **12**, 983–1000 (2021).
16. Chiossone, L. et al. Maturation of mouse NK cells is a 4-stage developmental program. *Blood* **113**, 5488–5496 (2009).
17. Fagundes, C. T. et al. Transient TLR activation restores inflammatory response and ability to control pulmonary bacterial infection in germfree mice. *J. Immunol.* **188**, 1411–1420 (2012).
18. Brown, R. L., Sequeira, R. P. & Clarke, T. B. The microbiota protects against respiratory infection via GM-CSF signaling. *Nat. Commun.* **8**, 1512 (2017).
19. Ichinohe T. et al. Microbiota regulates immune defense against respiratory tract influenza A virus infection. *Proc Natl Acad Sci USA*. **108**, 5354–5359 (2011).
20. Antunes, K. H. et al. Microbiota-derived acetate protects against respiratory syncytial virus infection through a GPR43-type 1 interferon response. *Nat. Commun.* **10**, 3273 (2019).
21. Doherty, T. M., Olsen, A. W., van Pinxteren, L. & Andersen, P. Oral vaccination with subunit vaccines protects animals against aerosol infection with Mycobacterium tuberculosis. *Infect. Immun.* **70**, 3111–3121 (2002).
22. KuoLee, R., Harris, G., Conlan, J. W. & Chen, W. Oral immunization of mice with the live vaccine strain (LVS) of Francisella tularensis protects

mice against respiratory challenge with virulent type A F. tularensis. *Vaccine* **25**, 3781–3791 (2007).
23. Samuelson, D. R. et al. Oral immunization of mice with live pneumocystis murina protects against pneumocystis pneumonia. *J. Immunol.* **196**, 2655–2665 (2016).
24. Samuelson, D. R. et al. Alcohol consumption increases susceptibility to pneumococcal pneumonia in a humanized murine HIV model mediated by intestinal dysbiosis. Alcohol **80**, 33–43 (2019).
25. Orange, J. S., Wang, B., Terhorst, C. & Biron, C. A. Requirement for natural killer cell-produced interferon gamma in defense against murine cytomegalovirus infection and enhancement of this defense pathway by interleukin 12 administration. *J. Exp. Med.* **182**, 1045–1056 (1995).
26. Tay, C. H., Szomolanyi-Tsuda, E. & Welsh, R. M. Control of infections by NK cells. *Curr. Top. Microbiol. Immunol.* **230**, 193–220 (1998).
27. Lodoen, M. B. & Lanier, L. L. Natural killer cells as an initial defense against pathogens. *Curr. Opin. Immunol.* **18**, 391–398 (2006).
28. Wesselkamper, S. C. et al. NKG2D is critical for NK cell activation in host defense against Pseudomonas aeruginosa respiratory infection. *J. Immunol.* **181**, 5481–5489 (2008).
29. Small, C. L. et al. NK cells play a critical protective role in host defense against acute extracellular Staphylococcus aureus bacterial infection in the lung. *J. Immunol.* **180**, 5558–5568 (2008).
30. Hall, L. J. et al. Natural killer cells protect against mucosal and systemic infection with the enteric pathogen Citrobacter rodentium. *Infect. Immun.* **81**, 460–469 (2013).
31. Ivin, M. et al. Natural killer cell-intrinsic type I IFN signaling controls Klebsiella pneumoniae growth during lung infection. *PLoS Pathog.* **13**, e1006696 (2017).
32. Feehan, D. D. et al. Natural killer cells kill extracellular Pseudomonas aeruginosa using contact-dependent release of granzymes B and H. *PLoS Pathog.* **18**, e1010325 (2022).
33. Cook, R. T. et al. Ethanol and natural killer cells. I. Activity and immunophenotype in alcoholic humans. *Alcohol Clin. Exp. Res.* **21**, 974–980 (1997).
34. Spitzer, J. H. & Meadows, G. G. Modulation of perforin, granzyme A, and granzyme B in murine natural killer (NK), IL2 stimulated NK, and lymphokine-activated killer cells by alcohol consumption. *Cell Immunol.* **194**, 205–212 (1999).
35. Zhang, H. & Meadows, G. G. Chronic alcohol consumption perturbs the balance between thymus-derived and bone marrow-derived natural killer cells in the spleen. *J. Leukoc. Biol.* **83**, 41–47 (2008).
36. Zhang, H., Zhu, Z. & Meadows, G. G. Chronic alcohol consumption decreases the percentage and number of NK cells in the peripheral lymph nodes and exacerbates B16BL6 melanoma metastasis into the draining lymph nodes. *Cell Immunol.* **266**, 172–179 (2011).
37. Tsay, T. B., Chen, P. H. & Chen, L. W. Aryl hydrocarbon receptor ligands enhance lung immunity through intestinal IKKbeta pathways. *J. Transl. Med.* **17**, 304 (2019).
38. Quintana, F. J. et al. Control of T(reg) and T(H)17 cell differentiation by the aryl hydrocarbon receptor. *Nature* **453**, 65–71 (2008).
39. Lee, J. S. et al. AHR drives the development of gut ILC22 cells and postnatal lymphoid tissues via pathways dependent on and independent of Notch. *Nat. Immunol.* **13**, 144–151 (2011).
40. Hughes, T. et al. Interleukin-1beta selectively expands and sustains interleukin-22+ immature human natural killer cells in secondary lymphoid tissue. *Immunity* **32**, 803–814 (2010).
41. Shin, J. H. et al. Modulation of natural killer cell antitumor activity by the aryl hydrocarbon receptor. *Proc. Natl Acad. Sci. USA* **110**, 12391–12396 (2013).
42. Cella, M. et al. A human natural killer cell subset provides an innate source of IL-22 for mucosal immunity. *Nature* **457**, 722–725 (2009).
43. Yu, J. et al. Pro- and antiinflammatory cytokine signaling: reciprocal antagonism regulates interferon-gamma production by human natural killer cells. *Immunity* **24**, 575–590 (2006).
44. Castriconi, R. et al. Transforming growth factor beta 1 inhibits expression of NKp30 and NKG2D receptors: consequences for the NK-mediated killing of dendritic cells. *Proc. Natl Acad. Sci. USA* **100**, 4120–4125 (2003).
45. Viel, S. et al. TGF-beta inhibits the activation and functions of NK cells by repressing the mTOR pathway. *Sci. Signal* **9**, ra19 (2016).
46. Poole, J. A. et al. Toll-like receptor 2 regulates organic dust-induced airway inflammation. *Am. J. Respir. Cell Mol. Biol.* **45**, 711–719 (2011).
47. Poole, J. A. et al. Intranasal organic dust exposure-induced airway adaptation response marked by persistent lung inflammation and pathology in mice. *Am. J. Physiol. Lung Cell Mol. Physiol.* **296**, L1085–L1095 (2009).

Acknowledgements

We would like to thank Paul Fey for providing the de-identified *K. pneumoniae* clinical isolates obtained from the Nebraska Medicine Clinical Microbiology Laboratory. This research was funded by the National Institutes of Health; the National Institute on Alcohol Abuse and Alcoholism Grants #R00-AA026336 (D.R.S.), #P50-AA030407 (T.A.W.), #F32 AA031180 (D.N.V.); the National Heart, Lung, and Blood Institute Grant #R01-HL156952 (DLK); the National Institute of Diabetes and Digestive and Kidney Diseases Grant #R01-DK131990-01 (D.R.S.); and the Nebraska University Foundation (D.R.S.). TAW is the recipient of a Research Career Scientist Award #IK6-BX005962 from the Department of Veterans Affairs. The content is solely the responsibility of the authors and does not necessarily represent the official views of the National Institutes of Health or the Department of Veterans Affairs. The funders had no role in study design, data collection and analysis, decision to publish, or preparation of the manuscript.

Author contributions

Conceptualization, D.R.S. (Derrick R. Samuelson), and D.N.V.; methodology, D.R.S. (Derrick R. Samuelson), D.R.S. (Deandra R. Smith), K.C.C., M.M., D.N.V., T.A.W., and D.L.K.; validation, D.R.S. (Derrick R. Samuelson), K.C.C., and D.N.V.; formal analysis, D.R.S. (Derrick R. Samuelson), D.R.S. (Deandra R. Smith), K.C.C., M.M., D.N.V.; resources, D.R.S. (Derrick R. Samuelson), T.A.W., and D.L.K.; data curation, K.C.C., D.N.V., M.M., D.R.S. (Derrick R. Samuelson), and D.R.S. (Deandra R. Smith); writing—original draft preparation, D.N.V., and D.R.S. (Derrick R. Samuelson); writing—review and editing, D.R.S. (Derrick R. Samuelson), D.R.S. (Deandra R. Smith), K.C.C., T.A.W., D.N.V., M.M., and D.L.K.; visualization, D.R.S. (Derrick R. Samuelson) and D.N.V.; supervision, D.R.S. (Derrick R. Samuelson); project administration, D.R.S. (Derrick R. Samuelson); funding acquisition, D.R.S. (Derrick R. Samuelson), T.A.W., and D.L.K. All authors have read and agreed to the published version of the manuscript.

Competing interests

The authors declare no competing interests.

Additional information

Supplementary information The online version contains supplementary material available at https://doi.org/10.1038/s41522-024-00558-w.

Correspondence and requests for materials should be addressed to Derrick R. Samuelson.